Journal of Materials Chemistry A

COMMUNICATION

View Article Online
View Journal | View Issue

Cite this: J. Mater. Chem. A, 2015, 3, 1920

Received 13th November 2014
Accepted 8th December 2014

DOI: 10.1039/c4ta06140c

www.rsc.org/MaterialsA

A versatile strategy to directly synthesize 4,8-functionalized benzo[1,2-*b*:4,5-*b*′]difurans for organic electronics†

Linyi Bian, Jiefeng Hai, Enwei Zhu, Jiangsheng Yu, Yun Liu, Jie Zhou, Guidong Ge and Weihua Tang*

A direct synthesis of 4,8-functionalized benzo[1,2-*b*:4,5-*b*′]difurans (BDFs) is developed. By fine-tuning the energy levels with different 4,8-functionalities or incorporating with electron-accepting units, BDFs show great potential as organic electronic materials, as demonstrated by 4.61% power conversion efficiency for polymer solar cells.

Organic semiconductors are attracting considerable interest because of their flexibility and easy structural modifications.[1–4] As one of the most important fused-ring structures, benzo[1,2-*b*:4,5-*b*′]dithiophene (BDT) is commonly explored as a π-electron donor in organic electronics such as organic field effect transistors, organic light-emitting diodes, as well as dye-sensitized and bulk heterojunction (BHJ) solar cells.[5,6] For example, BDT-based single-layer BHJ solar cells achieved a landmark power conversion efficiency of 9.2%.[6f] The BDT-based small molecule exhibited a hole mobility up to 0.81 $cm^2 V^{-1} s^{-1}$ in a single crystal transistor.[5]

In comparison to thiophene-based BDT, benzo[1,2-*b*:4,5-*b*′]-difuran (BDF) has attracted considerably less attention for organic electronics. However, BDF counterparts can harvest deeper HOMO and LUMO levels by replacing sulfur atoms in BDT with oxygen atoms, which are smaller in diameter but higher in electronegativity. BDF-based donor–acceptor (D–A) type copolymers have shown tighter packing and a smaller reorganization energy than their BDT counterparts, which could lead to a higher charge mobility and a smaller energy bandgap coupled with higher HOMO energy levels.[7] Furthermore, furan based materials also show improved solubilities, weaker steric hindrance, biodegradability and biorenewable properties.[8,9] Several BDF D–A copolymers were reported to deliver PCEs of 4–6% in BHJ solar cells when used as donors.[8–12] New interests in constructing structural hybrids of BDF and BDT, *i.e.*, thieno[2,3-*f*]benzofuran (TBF), even emerge because of their promising photovoltaic properties.[13] BDF unit has thus been regarded as an attractive building block in constructing D–A conjugated systems for various optoelectronic applications.

To date, the 4,8-functionalization of BDF has been explored by adopting similar approaches as for BDT with 4,8-dione as the precursor.[14,15] Starting from benzo[1,2-*b*:4,5-*b*′]difuran-4,8-dione, BDF monomers with alkyl, alkoxy, and aromatic rings substituted onto the benzene core were developed as donor units for D–A polymers.[17–21] However, the reported methods have certain drawbacks: (i) the methods employing either *n*-BuLi/$SnCl_2$ (ref. 15) and Grignard reagents[16] have quite limited options for substrates and are always accompanied by low yields; (ii) larger fused aromatic substituents could hardly be incorporated onto the benzene core due to steric hindrance.

In light of the ever-increasing interest in developing 2-dimensional (2D) aromatic fused ring structures to fine tune the energy levels and facilitate regular π–π stacking of conjugated molecules and polymer backbones, our group has recently developed an efficient synthetic route for the direct synthesis of 4,8-functionalized BDT monomers using 4,8-triflated BDT as the key prescusor.[17] However, the ring-closure formation of precursor BDT/BDF-4,8-dione requires harsh reaction conditions and gives low yields.

In this work, we present a general method for the direct synthesis of 4,8-functionalized BDF building blocks under mild reaction conditions (Scheme 1). By adopting the acid-catalysed furan arylation, 4,8-dibromobenzo[1,2-*b*:4,5-*b*′]difuran, demonstrates its versatility for the 4,8-functionalization of BDF to manipulate the energy levels of the resulted BDF monomers. This method paved the way for further bandgap engineering of BDF-based D–A copolymers.

A three-step protocol starting from hydroquinone facilely afforded the key synthon, 4,8-dibromobenzo[1,2-*b*:4,5-*b*′]-difuran (dibromo BDF), with an overall yield of 32% (see ESI†). As illustrated, 1,4-dibromo-2,5-bis(2,2-diethoxyethoxy)benzene

Key Laboratory of Soft Chemistry and Functional Materials (Ministry of Education of China), Nanjing University of Science and Technology, Nanjing 210094, China. E-mail: whtang@mail.njust.edu.cn; Fax: +86-25-8431-7311; Tel: +86-25-8431-7311

† Electronic supplementary information (ESI) available: Experimental procedure and characterization for new materials, as well as device fabrication and characterization. See DOI: 10.1039/c4ta06140c

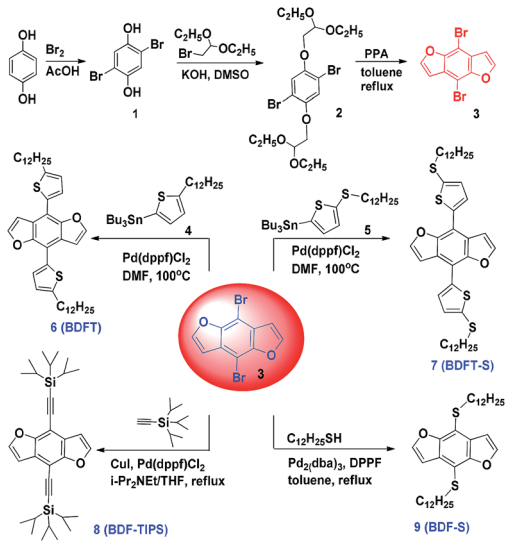

Scheme 1 Synthetic route to 4,8-functionalized BDF monomers with 4,8-dibromobenzo[1,2-*b*:4,5-*b*′]difuran as a versatile synthon.

2 was synthesized using Williamson-etherification between 2,5-dibromobenzene-1,4-diol **1** and 2-bromo-1,1-diethoxyethane with an overall yield above 80%. A further cyclocondensation of **2** using polyphosphoric acid (PPA) as acid catalyzed agent afforded 4,8-dibromobenzo[1,2-*b*:4,5-*b*′]difuran **3** with 60% yield. The replacement of PPA with Amberlyst-15 resin to increase the yield did not work as expected, probably due to the slow reaction kinetics and aromaticity.[18]

With dibromo BDF **3** in hand, a wide variety of 4,8-functionalized BDF monomers could be readily prepared using palladium-catalyzed Stille and Sonogashira coupling as well as carbon–sulfur formation reactions with high yields (≥86%). Dialkylthio substituted BDFs were prepared *via* a straightforward carbon–sulfur bond formation reaction, which was previously afforded *via* high-temperature Newman–Kwart rearrangement reaction using irritant reagents.[19]

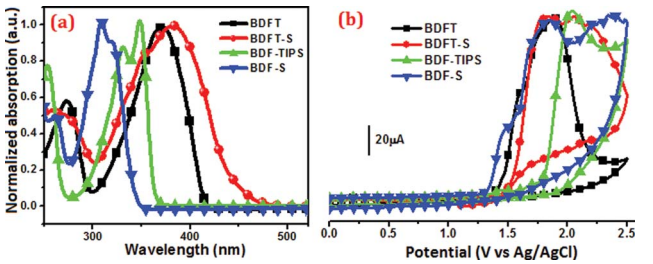

Fig. 1 (a) Normalized absorption spectra of BDF monomers in $CHCl_3$ solutions, (b) cyclic voltammogram of BDF monomers in solutions.

To demonstrate the versatility of this approach, both electron donating (alkylthio, aromatic ring) and accepting units (triisopropylsilylethynyl) were explored for the 4,8-functionalization of BDF. The Stille cross-coupling between dibromo BDF and 2-dodecyl-5-tributyltinthiophene or 2-dodecylthio-5-tributyltinthiophene[20] proceeded efficiently to afford new BDF monomers **6** (BDFT) and **7** (BDFT-S) in 90% and 87% yield, respectively. The dibromo BDF was also explored for Sonogashira coupling with (triisopropylsilyl)acetylene in the presence of bis(triphenylphosphine) palladium(II) dichloride and cuprous iodide as the catalyst to afford triisopropylsilyl ethynyl-substituted **8** (BDF-TIPS) with a yield of 90%. The dialkylthio **9** (BDF-S) was easily prepared *via* C–S cross-coupling[20] under the catalysis of $Pd_2(dba)_3$ and DPPF (1,1′-bis(diphenylphosphino)-ferrocene) ligand with 95% yield.

The absorption spectra of BDF monomers in chloroform solution are plotted in Fig. 1 (thin films shown in Fig. S1†). In solution, four BDF monomers BDFT, BDFT-S, BDF-TIPS and BDF-S showed an absorption peak (λ_{max}) at 371 nm, 382 nm, 348 nm and 308 nm, respectively (Table 1). BDF-TIPS and BDF-S displayed two shoulder peaks at 331 nm and 321 nm. In the solid state, BDF monomers displayed similar absorption profiles but extended absorption, indicating the increased intermolecular interactions and aggregation. The red-shifted

Table 1 Optical and electrochemical properties of BDF monomers

	UV-vis					CV		
	$\lambda_{max}{}^a$ (nm)	$\lambda_{onset}{}^a$ (nm)	$\lambda_{max}{}^b$ (nm)	$\lambda_{onset}{}^b$ (nm)	E_g^{optc} (eV)	E_{onset}^{ox} (V)	HOMO^d (eV)	LUMO^e (eV)
BDFT	371	414	375	419	2.96	1.36	−5.76	−2.80
BDFT-S	382	474	388	480	2.58	1.42	−5.82	−3.24
BDF-TIPS	348	367	351	369	3.36	1.35	−5.75	−2.39
BDF-S	308	351	312	354	3.50	1.28	−5.68	−2.18
P1	693	905	709	973	1.27	0.71	−5.11	−3.84
P2	712	951	744	1016	1.22	0.69	−5.09	−3.87
P3	701	906	708	942	1.32	0.78	−5.18	−3.86
P4	696	929	715	970	1.28	0.75	−5.15	−3.87
P5	902	—	945	—	—	0.47	−4.87	—
P6	851	—	947	—	—	0.60	−5.00	—
P7	795	—	853	—	—	0.76	−5.16	—
P8	945	—	981	—	—	0.62	−5.02	—
P9	559	666	570	730	1.70	0.91	−5.31	−3.61

[a] Absorption in solution. [b] Absorption in film. [c] $E_g^{opt} = 1240/\lambda_{onset}$. [d] HOMO = −e($E_{onset}^{ox}$ + 4.4) (eV). [e] LUMO = HOMO + E_g^{opt}.

absorption spectra followed the order of BDF-S < BDF-TIPS < BDFT < BDFT-S.

The optical results of BDF-TIPS and BDF-S reveal that the introduction of a TIPS-ethynyl substituent to BDF core instead of alkylthio leads to a ~40 nm red-shifted absorption spectra, mainly due to the expanded conjugated system and the electron-withdrawing effect of TIPS-ethynyl group. In comparison to BDF-S and BDF-TIPS, BDFT-S and BDFT show a more red-shifted absorption, suggesting an enhanced electron delocalization over 2D conjugated BDF moieties when substituted with aromatic functionalities. BDFT-S exhibited ~11 nm red-shifted absorption than BDFT when BDF was substituted with alkylthiothienyl instead of alkylthienyl group. As known, the longer wavelength domain corresponds to the π–π* transition, dominated by the electron excitation from HOMO to LUMO. Based on the onset of the lowest energy absorption bands (λ_{onset}) of the films,[21] the corresponding optical bandgap (E_g^{opt}) of the BDF monomers was estimated to be in the range of 2.58–3.50 eV (Table 1).

When the λ_{max} values of three TIPS-ethynyl-substituted benzodichalcogenophenes are compared, we can find that BDF-TIPS exhibits a greater blue-shifted λ_{max} (351 nm) than TBF-TIPS (366 nm)[13] and BDT-TIPS (384 nm).[13] This indicates that the lower energy transition was significantly shifted with the increasing number of heavier chalcogen atoms, probably because the electronegativity of the heteroatom (O, 3.5; S, 2.5) play a fundamental role in the location of absorption maxima.[13] Comparing the absorption peak of BDF-S with that of BDT-S,[17] obvious red-shifts from 308 nm to 355 nm were found for their chloroform solutions. Similar phenomena were also found for the optical spectra of BDFT and BDTT[17] films. The more S atoms were incorporated into the benzodichalcogenophenes, the more the absorption red-shifted.

The electrochemical properties of the as-prepared BDF monomers were investigated by cyclic voltammetry (Fig. 1b). All the BDF monomers underwent an irreversible oxidation, similar to TBF and BDT monomers.[13,17] The onset potential for oxidation (E_{onset}^{ox}) was observed to be 1.36, 1.42, 1.35 and 1.28 V for BDFT, BDFT-S, BDF-TIPS and BDF-S, respectively. From E_{onset}^{ox}, the HOMO levels of derivatives were thus calculated (Table 1). The LUMO levels of BDF monomers were further determined in the range of −5.82–5.68 eV with their corresponding E_g^{opt} and HOMO energy levels. According to the data for BDFT and BDFT-S in Table 1, the 4,8-functionalization of the BDF core with alkylthienyl and alkylthiothienyl substituents proved to be more effective in lowering both LUMO and HOMO energy levels because the incorporated aromatic moieties enhanced the planarity to induce more effective π-electron delocalized conjugated systems. Compared with BDFT, alkylthio-substituted BDFT-S maintained even lower energy levels and wider absorption region due to the electron-donating effect of alkylthio group and enlarged conjugation.

Compared with BDF-S, BDF-TIPS displayed both lower LUMO and HOMO energy levels, which indicated that increased conjugation length and planarity were induced with the introduced triple bonds. For TIPS-ethynyl-substituted benzodichalcogenophene anologues, the HOMO level increased in the order of BDF (−5.75 eV) < TBF (−5.70 eV) < BDT (−5.58 eV), as a result of higher electronegativity of oxygen atom.[10,13] A deeper HOMO level was also observed for BDF monomers, when dialkylthio substituted BDF-S (−5.68 eV) was compared with BDT-S (−5.41 eV) and BDFT (−5.76 eV) with BDTT (−5.42).[17]

To explore the potential of these BDF monomers with finely-tuned energy levels for optoelectronic applications, BDF-based D–A copolymers were prepared by alternating with diketopyrrolopyrrole (DPP),[4,22] thiadiazolo[3,4-*g*]quinoxaline (BTQx)[23] and thiazolo[5,4-*d*]thiazole (TTz)[24] *via* the Stille coupling reaction (Scheme 2). DPP and TTz were selected due to their moderate electro-withdrawing ability to build narrow bandgap conjugated materials (*ca.*, 1.5–2.0 eV), whereas stronger accepting BTQx units have been explored for organic semiconductors with extremely low bandgaps (*ca.* 1.0–1.5 eV) for near infrared optoelectronics.[25]

With BDF tin reagents **10–13** (Scheme 2) in hand, structurally well-defined alternating polymers **P1–P9** were synthesized for BHJ solar cell applications. All the polymers showed excellent solubility in common organic solvents and had relatively high molecular weights (M_n = 9.6–41.7 kDa) (Table S1†). The thermogravimetric analysis (TGA) revealed the excellent thermal stability of polymers **P1–P9**, with T_d (temperature correspond to 5% weight loss) ranging from 320 °C to 423 °C (Fig. S2†).

The BDF polymers **P1–P9** exhibited strongly acceptor-dependent photophysical and electronic properties (Table 1 and Fig. 2). DPP-based **P1–P4** exhibited strong absorption at 550–850 nm in films (Fig. S3†), with E_g^{opt} calculated to be range from 1.22 eV to 1.32 eV. BTQx-based polymers **P5–P8** showed a typical two-absorption-band profile (Fig. S4†), *i.e.*, one at 300–600 nm and the other extending from 600 nm to the near-infrared region (>1100 nm), which endowed extremely narrow E_g^{opt} values (≤1.13 eV) for **P5–P8**. TTz-based **P9** exhibited one intensified absorption band at 400–650 nm. All the polymers exhibited HOMO levels ranging from −4.87 to −5.31 eV and LUMO levels

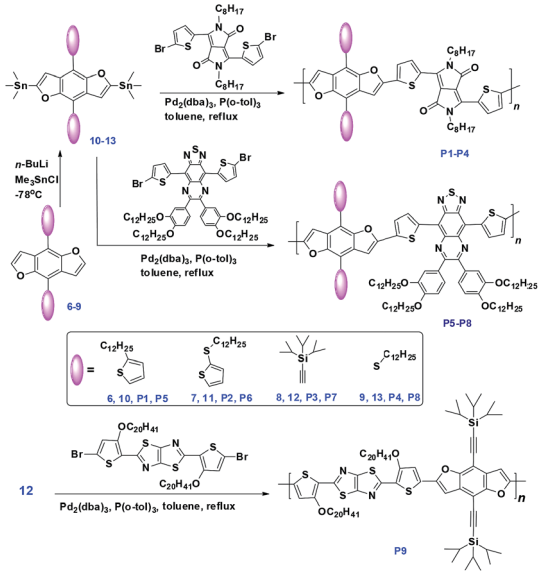

Scheme 2 Synthetic route to BDF-based D–A polymers.

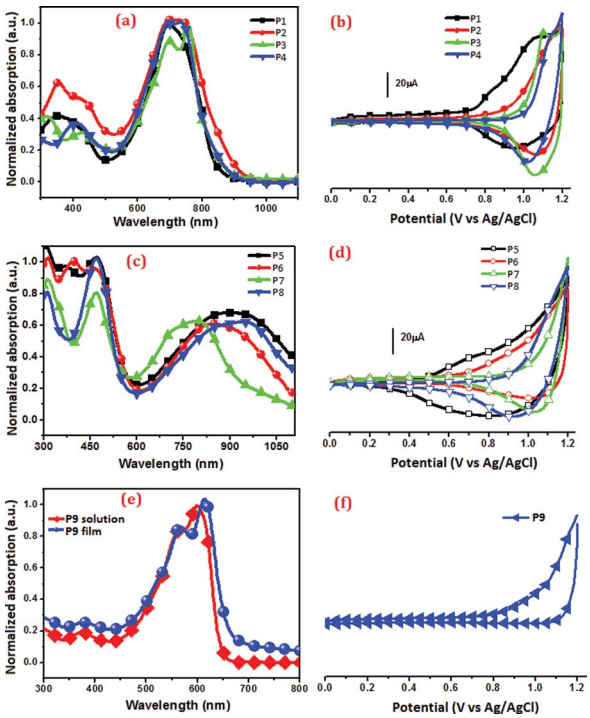

Fig. 2 Normalized absorption spectra of (a) **P1**–**P4**, (c) **P5**–**P8** and (e) **P9** in $CHCl_3$ solutions. CV traces of (b) **P1**–**P4**, (d) **P5**–**P8** and (f) **P9**.

from −3.61 to −3.87 eV. As shown, the bandgaps as well as the molecular electronic energy levels of BDF-cored polymers are readily tuned by copolymerizing with accepting units with different electron-withdrawing capability, in the order of TTz < DPP < BTQx in our case.

The photovoltaic potential of BDF polymers were explored using the conventional single-layer device with a configuration of ITO/PEDOT:PSS/**P9**:PCBM (1 : 2, w/w)/LiF/Al (Table 2 and Fig. 3). The blend films of both **P9**:$PC_{61}BM$ and **P9**:$PC_{71}BM$ spin-coated from the corresponding chlorobenzene solutions acted as the photoactive layers. The preliminary study revealed that **P9**:$PC_{61}BM$ device delivered power conversion efficiencies (PCEs) up to 2.29% under AM1.5 illumination (100 mW cm^{-2}), whereas the **P9**:$PC_{71}BM$ device exhibited a maximum PCE of 2.63%. The devices were further optimized by spin-coating **P9**:$PC_{71}BM$ solution with the addition of 5% DIO. The best devices delivered a PCE of 4.61%, with a V_{oc} of 0.80 V, a J_{sc} of 9.81 mA cm^{-2} and a FF of 58.7%. The photovoltaic performances of BDT counterpart polymer solar cells delivered the highest PCE of 4.33%, with a J_{sc} of 9.77 mA cm^{-2}, a V_{oc} of 0.89 V, and a FF of 49.8%.[26] The higher FF may be attributed to the

Table 2 Key photovoltaic parameters of polymer : PCBM (1 : 2, w/w) PSCs

Device	V_{oc} (V)	J_{sc} (mA cm^{-2})	FF (%)	PCE (%)
P9:$PC_{61}BM$	0.83	6.12	45.4	2.29
P9:$PC_{71}BM$	0.80	7.51	43.8	2.63
P9:$PC_{71}BM$ (with 5% DIO)	0.80	9.81	58.7	4.61

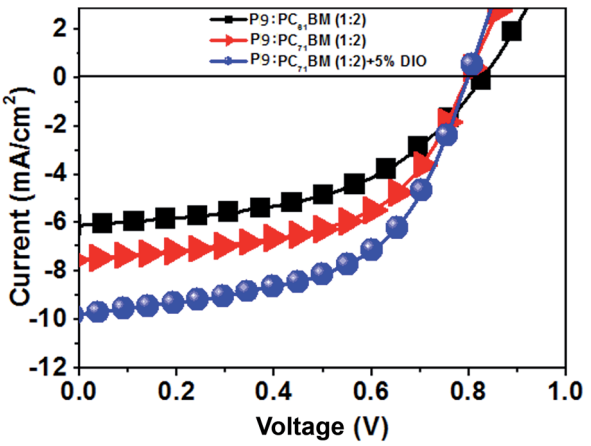

Fig. 3 *J*–*V* characteristics of ITO/PEDOT:PSS/**P9**:PCBM (1 : 2, w/w)/LiF/Al devices under the irradiation of AM1.5 G (100 mW cm^{-2}).

smaller diameter but higher electronegativity of oxygen atom. Our model BDF polymers are very attractive for photovoltaic applications. The relatively lower J_{sc} and FF, we believe, can be optimized with device engineering. The characterization of photovoltaic properties for polymers **P1**–**P8** with stronger accepting units (BTQx and DPP) is in progress and will be reported in due time.

In conclusion, we presented a versatile synthetic strategy for 4,8-functionalized BDF building blocks using 4,8-dibromobenzo[1,2-*b*:4,5-*b*′]difuran as a versatile synthon. A platform is provided for feasible late-stage BDF derivatization. The chalcogen-property correlation study reveals a narrowing bandgap and lowering of energy levels on going from sulfur to oxygen. BDF-based polymers with fine-tuned absorption and energy levels exhibit promising potential for solar cells with a PCE of 4.61%, demonstrated in initial testing. As a consequence, the present work provides an insight on the structure–property relationship of BDF based conjugated materials and opens an avenue to develop a new library of extended π-conjugated BDF molecules/polymers with high structural diversity for optoelectronic applications.

Acknowledgements

This work is supported by the National Natural Science Foundation of China (Grant no. 21074055), Program for New Century Excellent Talents in University (NCET-12-0633), Jiangsu Province Natural Science Fund for Distinguished Young Scholars (BK20130032), Doctoral Fund of Ministry of Education of China (no. 20103219120008), and the Fundamental Research Funds for the Central Universities (30920130111006).

Notes and references

1 C. K. Chiang, C. R. Fincher, Y. W. Park, A. J. Heeger, H. Shirakawa, E. J. Louis, S. C. Gau and A. G. MacDiarmid, *Phys. Rev. Lett.*, 1977, **39**, 1098.

2 C. Wang, H. Dong, W. Hu, Y. Liu and D. Zhu, *Chem. Rev.*, 2012, **112**, 2208.
3 L. Xie, C. Yin, W. Lai, Q. Fan and W. Huang, *Prog. Polym. Sci.*, 2012, **37**, 1192.
4 L. Bian, E. Zhu, J. Tang, W. Tang and F. Zhang, *Prog. Polym. Sci.*, 2012, **37**, 1292.
5 S. Wang, S. Ren, Y. Xiong, M. Wang, X. Gao and H. Li, *ACS Appl. Mater. Interfaces*, 2013, **5**, 663.
6 (*a*) D. H. Lee, J. Shin, M. J. Cho and D. H. Choi, *Chem. Commun.*, 2013, **49**, 3896; (*b*) H. Pan, Y. Li, Y. Wu, P. Liu, B. S. Ong, S. Zhu and G. Xu, *J. Am. Chem. Soc.*, 2007, **129**, 4112; (*c*) S. Holliday, J. E. Donaghey and I. McCulloch, *Chem. Mater.*, 2014, **26**, 647; (*d*) P. M. Beaujuge and J. M. J. Fréchet, *J. Am. Chem. Soc.*, 2011, **133**, 20009; (*e*) L. Dou, J. You, J. Yang, C.-C. Chen, Y. He, S. Murase, T. Moriarty, K. Emery, G. Li and Y. Yang, *Nat. Photonics*, 2012, **6**, 180; (*f*) Z. He, C. Zhong, S. Su, M. Xu, H. Wu and Y. Cao, *Nat. Photonics*, 2012, **6**, 591; (*g*) J. You, L. Dou, Z. Hong, G. Li and Y. Yang, *Prog. Polym. Sci.*, 2013, **38**, 1909; (*h*) E. Wang, W. Mammo and M. R. Andersson, *Adv. Mater.*, 2014, **26**, 1801.
7 For selected examples: (*a*) U. H. F. Bunz, *Angew. Chem., Int. Ed.*, 2010, **49**, 5037; (*b*) H. Tsuji, C. Mitsui, L. Ilies, Y. Sato and E. Nakamura, *J. Am. Chem. Soc.*, 2007, **129**, 11902; (*c*) H. Tsuji, C. Mitsui, Y. Sato and E. Nakamura, *Adv. Mater.*, 2009, **21**, 3776.
8 C. Hu, Y. Fu, S. Li, Z. Xie and Q. Zhang, *Polym. Chem.*, 2012, **3**, 2949.
9 L. Huo, L. Ye, Y. Wu, Z. Li, X. Guo, M. Zhang, S. Zhang and J. Hou, *Macromolecules*, 2012, **45**, 6923.
10 B. Liu, X. Chen, Y. Zou, L. Xiao, X. Xu, Y. He, L. Li and Y. Li, *Macromolecules*, 2012, **45**, 6898.
11 (*a*) X. Chen, B. Liu, Y. Zou, L. Xiao, X. Guo, Y. He and Y. Li, *J. Mater. Chem.*, 2012, **22**, 17724; (*b*) B. Liu, B. Qiu, X. Chen, L. Xiao, Y. Li, Y. He, L. Jiang and Y. Zou, *Polym. Chem.*, 2014, **5**, 5002; (*c*) B. Liu, X. Chen, Y. Zou, Y. He, L. Xiao, X. Xu, L. Li and Y. Li, *Polym. Chem.*, 2013, **4**, 470.
12 L. Huo, Y. Huang, B. Fan, X. Guo, Y. Jing, M. Zhang, Y. Li and J. Hou, *Chem. Commun.*, 2012, **48**, 3318.
13 Y. Aeschi, H. Li, Z. Cao, S. Chen, A. Amacher, N. Bieri, B. Özen, J. Hauser, S. Decurtins, S. Tan and S. Liu, *Org. Lett.*, 2013, **15**, 5586.
14 (*a*) P. Beimling and G. Kobmehl, *Chem. Ber.*, 1986, **119**, 3198; (*b*) H. Pan, Y. Li, Y. Wu, P. Liu, B. S. Ong, S. Zhu and G. Xu, *Chem. Mater.*, 2006, **18**, 3237.
15 J. Hou, M.-H. Park, S. Zhang, Y. Yao, L.-M. Chen, J.-H. Li and Y. Yang, *Macromolecules*, 2008, **41**, 6012.
16 (*a*) L. Dou, J. Gao, E. Richard, J. You, C.-C. Chen, K. C. Cha, Y. He, G. Li and Y. Yang, *J. Am. Chem. Soc.*, 2012, **134**, 10071; (*b*) J. Yuan, L. Xiao, B. Liu, Y. Li, Y. He, C. Pan and Y. Zou, *J. Mater. Chem. A*, 2013, **1**, 10639.
17 E. Zhu, G. Ge, J. Shu, M. Yi, L. Bian, J. Hai, J. Yu, Y. Liu, J. Zhuo and W. Tang, *J. Mater. Chem. A*, 2014, **2**, 13580.
18 (*a*) C. J. Moody, K. J. Doyle, M. C. Elliott and T. J. Mowlem, *J. Chem. Soc., Perkin Trans. 1*, 1997, 2413; (*b*) N. Brown and K. R. Buszek, *Tetrahedron Lett.*, 2012, **53**, 4022.
19 D. Lee, S. W. Stone and J. P. Ferraris, *Chem. Commun.*, 2011, **47**, 10987.
20 T. Okauchi, K. Kuramoto and M. Kitamura, *Synlett*, 2010, **19**, 2891.
21 W. Tang, L. Ke, L. Tan, T. Lin, T. Kietzke and Z.-K. Chen, *Macromolecules*, 2007, **40**, 6164.
22 (*a*) M. Kaur and D. H. Choi, *Chem. Soc. Rev.*, 2015, **44**, 58–77; (*b*) B. Walker, J. Liu, C. Kim, G. C. Welch, J. K. Park, J. Lin, P. Zalar, C. M. Proctor, J. H. Seo, G. C. Bazan and T.-Q. Nguyen, *Energy Environ. Sci.*, 2013, **6**, 952–962.
23 (*a*) J. Hai, W. Yu, E. Zhu, L. Bian, J. Zhang and W. Tang, *Thin Solid Films*, 2014, **562**, 75; (*b*) J. Hai, G. Shi, J. Yu, E. Zhu, L. Bian, W. Ma and W. Tang, *New J. Chem.*, 2014, **38**, 4816.
24 J. Hai, B. Zhao, F. Zhang, C.-X. Sheng, L. Yin, Y. Li, E. Zhu, L. Bian, H. Wu and W. Tang, *Polymer*, 2013, **54**, 4930.
25 (*a*) T. L. Tam, H. Li, Y. M. Lam, S. G. Mhaisalkar and A. C. Grimsdale, *Org. Lett.*, 2011, **13**, 4612; (*b*) M. Sun, L. Wang, X. Zhu, B. Du, R. Liu, W. Yang and Y. Cao, *Sol. Energy Mater. Sol. Cells*, 2007, **91**, 1681; (*c*) G. Qian, Z. Zhong, M. Luo, D. Yu, Z. Zhang, D. Ma and Z. Y. Wang, *J. Phys. Chem. C*, 2009, **113**, 1589.
26 Q. Shi, H. Fan, Y. Liu, W. Hu, Y. Li and X. Zhan, *Macromolecules*, 2011, **44**, 9173.

